

**THE STRUCTURE OF THE SOUND FIELD FOR A ROUND
CYLINDER PLACED INTO A HIGH-SPEED FLOW: DNS
APPROACHES IN THE 2D CASE**

M.A. Sumbatyan*, Marc Terracol**

**Faculty of Mathematics, Mechanics and Computer Science
South Federal University, Milchakova Street 8a
344090 Rostov-on-Don, Russia
Email: sumbat@math.rsu.ru*

***ONERA, Departement de Simulation Numerique des Ecoulements et Aeroacoustique
BP 72, 92322 Chatillon Cedex, France
Email: marc.terracol@onera.fr*

Key words: high-speed flow, Green's function, laminar flow, turbulent flow, Large-Eddy simulation, Direct Numerical simulation, round cylinder.

Abstract. In the present work we develop and compare two different approaches to calculate numerically the structure of the 2D sound field arising around a circular cylinder placed in a high-speed homogeneous stream of a viscous fluid. We start with the computations for a relatively low value of the Reynolds number, which corresponds to a 2D laminar flow. For that purpose, a DNS solver with high-order FD schemes and explicit time integration has been used. Then we develop a semi-analytical approach to treat directly turbulent flows around the cylinder. By using an implicit integration with respect to time, a standard BEM technique reduces the problem to a simple integration over the chosen domain. This is attained efficiently by applying a special form of the Green's function permitting separation of variables. The latter reduces essentially the "mesh" dimension of the algorithm.

**1. THE LIGHTHILL-CURLE AEROACOUSTIC THEORY AND THE
STRUCTURE OF THE TRANSIENT VELOCITY FIELD**

In his fundamental work¹ Lighthill laid the foundations of a new aeroacoustic theory starting from governing equations of viscous gas. The leading term defining acoustic pressure p can be determined from the following Lighthill equation

$$\frac{1}{c_0^2} \frac{\partial^2 p}{\partial t^2} - \nabla^2 p = \frac{\partial^2 T_{ij}}{\partial y_i \partial y_j}, \quad T_{ij} \approx \rho_0 v_i v_j \quad (1.1)$$

where c_0 is the wave speed in the medium, ρ_0 is the mass density, t is time, $\{y_i\}$ are Cartesian coordinates, and $\{v_i\}$ are the components of the velocity vector. Later Curle² developed the Lighthill theory to the case when the acoustic medium contains some rigid boundaries. It is clear from Eq. (1.1) that the sound generated aerodynamically is

defined by a certain wave equation with a source field given by the Lighthill's tensor T_{ij} . The latter is expressed as a combination of components of the velocity vector. It thus becomes clear that the aerodynamic sound can arise only in non-stationary (transient) flows, i.e. when the structure of the velocity field varies in time. Therefore, the key point of any aeroacoustic theory is a correct calculation of the velocity field as a function of time.

Let us consider a rigid round cylinder placed into a high-speed flow of viscous incompressible fluid (see Figure 1).

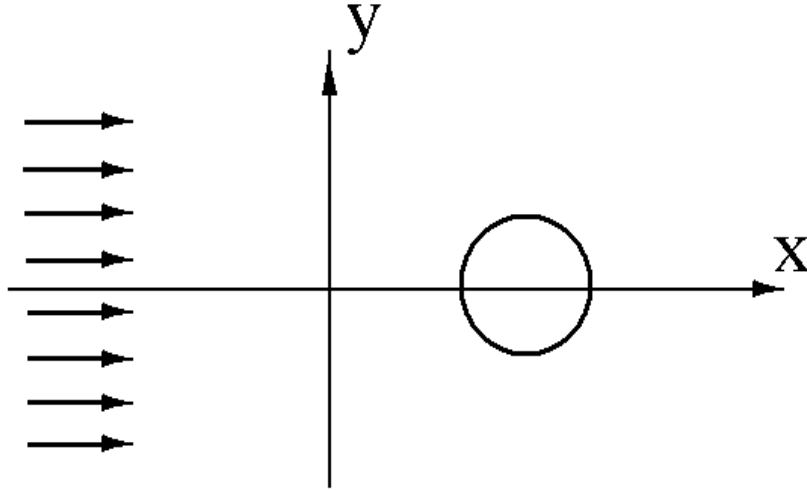


Figure 1. Homogeneous flow of a viscous fluid past a round cylinder

In the case of a laminar flow one can resort on classical numerical techniques to predict the flowfield. The next section presents an example of such a simulation

2. DNS OF THE LAMINAR FLOW AROUND A CYLINDER

2.1. Numerical method

The set of the three-dimensional unsteady filtered Navier-Stokes equations is solved using a structured multi-block solver, developed at ONERA for aeroacoustic studies^{3, 4, 5, 6}. The present simulations have been carried out using a set of high-order schemes, which are well suited for both aerodynamic and acoustic problems. The spatial scheme used in this study relies on a classical sixth-order accurate finite-difference centered discretization. The spatial derivatives of any quantity f are then computed as (in one dimension):

$$\frac{\partial f}{\partial x}(x) = \frac{1}{\Delta x} \sum_{k=-3}^3 a_k f(x + k\Delta x)$$

where Δx is the space step in the x -direction. The coefficients values are, respectively, $a_0 = 0$, $a_1 = -a_{-1} = 45/60$, $a_2 = -a_{-2} = 9/60$, $a_3 = -a_{-3} = 1/60$. A Fourier analysis of this scheme shows that eight points per wavelength are necessary for a satisfactory approximation of the derivative operator. For curvilinear grids, the curvilinear extension strategy proposed by Visbal and Gaitonde⁷ has been retained.

Since this centered scheme is non-dissipative, it promotes the growth of spurious high-frequency numerical errors. For this reason, a stabilization step is also added in the numerical method, which relies on the application of a tenth-order accurate centered linear filtering operator on the solution at each time step. This filtering operator F is defined as (in one dimension):

$$F(f)(x) = \frac{1}{\Delta x} \sum_{k=-5}^5 b_k f(x + k\Delta x)$$

The filter coefficient values are respectively: $b_0 = 772/1024$, $b_1 = b_{-1} = 210/1024$, $b_2 = b_{-2} = -120/1024$, $b_3 = b_{-3} = 45/1024$, $b_4 = b_{-4} = -10/1024$, $b_5 = b_{-5} = 1/1024$.

On uniform Cartesian grids, the filtering operator in two or three dimensions is simply obtained by recursive application of the filter in each direction.

Finally, time advancement is performed using a third order accurate explicit Runge-Kutta scheme with a maximum CFL number of 0.95 for the simulations presented in this study.

2.2. Computational setup

The incoming flow has a uniform speed $U_\infty = 70m/s$, and the diameter of the cylinder d is only set to $2 \cdot 10^{-5}m$, such that the associated Reynolds number remains only $Re=100$, therefore yielding to a 2D laminar flow around the cylinder and in its wake.

Two-dimensional computational grids have been considered. The computational domain extends to $200d$ away from the cylinder axis in the streamwise (x) and vertical (y) directions, the grid resolution making it possible to resolve correctly the acoustic waves associated to the fundamental vortex shedding frequency up to $100d$ away from the cylinder. A radial stretching of the mesh is used, such that the smallest cell at the cylinder surface corresponds to a radial step of $5 \cdot 10^{-3}d$, while ensuring a proper resolution of the acoustic waves up to $100d$. The azimuthal discretization uses 290 grid points, with also grid stretching applied such that the discretization in the rear part of the cylinder is finer than in the front one. The overall number of points used is slightly larger than 260,000. Figure 2 displays a close view of the mesh near the cylinder. It can be observed that this mesh is decomposed into six different blocks.

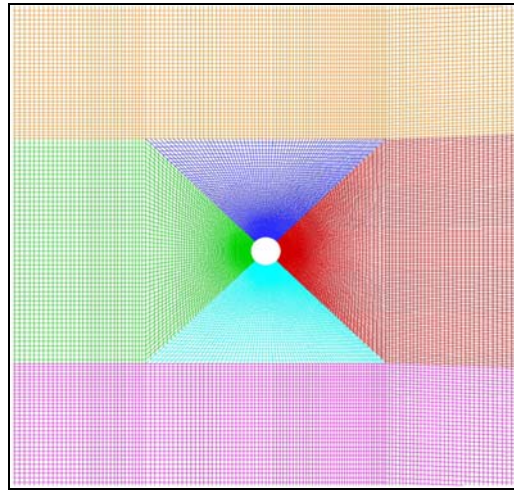


Figure 2. Close view of the mesh near the cylinder.

2.3. Results

All the results presented below are extracted after a sufficient transient time after which a statistical steady state of the flow is reached.

Figure 3 presents a two-dimensional visualization of the flow around the cylinder. It is observed that 2D vortices occur, forming the well-known Karman vortex street behind the cylinder. It can be checked that the use of a sixth-order accurate scheme makes it possible to represent correctly the wake physics far downstream of the cylinder, without involving a too fine grid resolution.

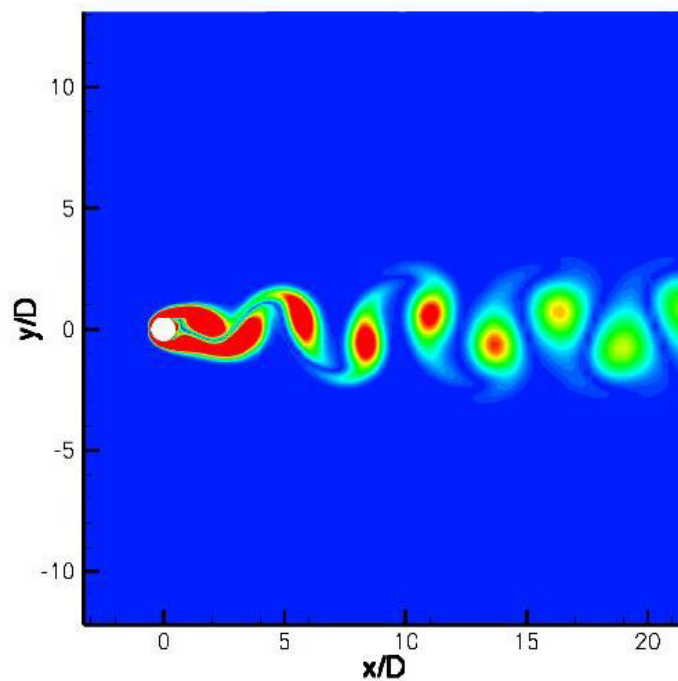


Figure 3. Two-dimensional view of the flow (iso-norm of vorticity contours).

Figure 4 displays 2D snapshots of isocontours of the dilatation field $\theta = \nabla \cdot u$, which makes it possible to highlight the circular acoustic waves emitted at the cylinder. The first observation is that the main sound source seems to act as a dipole. The associated pressure spectrum, computed at a distance of four diameters from the cylinder's axis, exhibits a main peak at a Strouhal number of about $St=0.164$, and several harmonics indicating that non linear interactions occur.

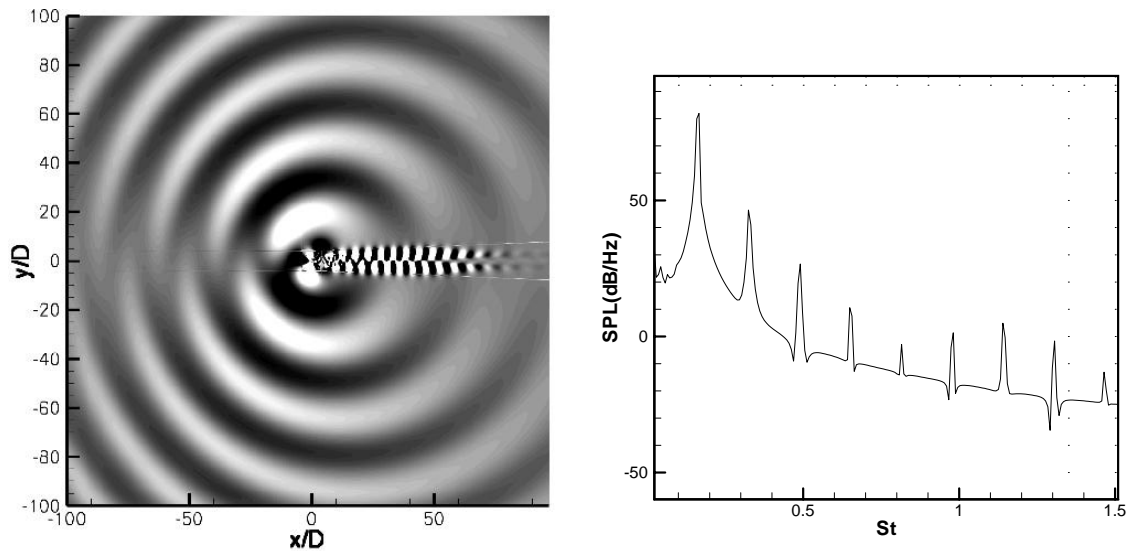


Figure 4. Left: Acoustic waves visualization (dilatation field). Right: pressure spectrum computed at 4 diameters from the cylinder's axis.

The DNS performed in this section shows that for low values of the Reynolds number, a detailed description of both the aerodynamic and acoustic features of the flow around a cylinder can be obtained. However, even for a low value of the Reynolds number, huge CPU resources are required when using classical numerical approaches. This is why they remain in general limited to laminar flows. The unsteady simulation of turbulent flows then generally requires to rely on modeling approaches such as LES, see for instance the work done in⁸.

In the next section, an alternative approach is therefore proposed to perform DNS at lower costs.

3. THE CASE OF TURBULENT FLOW

In order to predict a turbulent structure of the velocity field in high-speed flows, we develop here a new semi-analytical DNS method which can uniformly solve both laminar (less rapid flows) and turbulent (higher rapid flows). Then one can place a cylinder in the constructed turbulent flow. The structure of the turbulent flow is constructed in an imaginary channel of a constant width b . Then one can place a cylinder in the constructed turbulent flow (see Figure 5). The key merit of the proposed method is that it reduces significantly the number of arithmetic operations, therefore this permits application to extremely high flow speed.

The Navier-Stokes equations written in terms of vorticity ζ and stream function ψ has the following form

$$\frac{\partial \zeta}{\partial t} = -\mathbf{u} \frac{\partial \zeta}{\partial x} - \mathbf{v} \frac{\partial \zeta}{\partial y} + \nu \Delta \zeta, \quad \zeta = \Delta \psi, \quad (3.1)$$

where ν is the kinematic viscosity. The components of the velocity vector are

$$\mathbf{u} = \frac{\partial \psi}{\partial y}, \quad \mathbf{v} = -\frac{\partial \psi}{\partial x}, \quad \zeta = \frac{\partial \mathbf{u}}{\partial y} - \frac{\partial \mathbf{v}}{\partial x}. \quad (3.2)$$

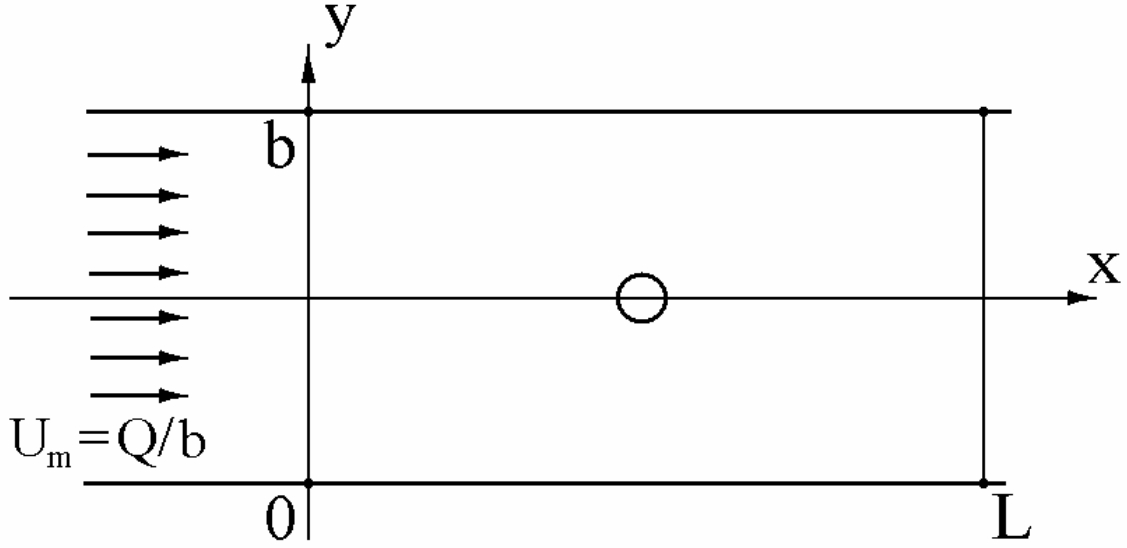


Figure 5. Round cylinder in a turbulent channel flow with a typical reference domain

Any implicit iteration scheme over time leads to a system of linear second-order elliptic equations for ζ and ψ

$$\begin{aligned} \zeta^{(n)} - \varepsilon \Delta \zeta^{(n)} &= g^{(n-1)}, & \Delta \psi^{(n)} &= \zeta^{(n)}, \\ \psi^{(n)}(x, 0) &= 0, \quad \psi^{(n)}(x, b) = Q, & \frac{\partial \psi^{(n)}}{\partial y}(x, b) &= \frac{\partial \psi^{(n)}}{\partial y}(x, b) = 0, \\ (\zeta, \psi)(0, \eta) &= (\zeta, \psi)(L, \eta), & \frac{\partial(\zeta, \psi)}{\partial \xi}(0, \eta) &= \frac{\partial(\zeta, \psi)}{\partial \xi}(L, \eta), \end{aligned} \quad (3.3)$$

where the periodic condition over horizontal coordinate is assumed to be valid, - a condition which is correct if the reference domain is sufficiently long: $L/b \gg 1$. Function $g^{(n-1)}$ represents a certain non-linear combination of some functions known from the previous iteration step.

The both second-order equations (3.3) for ζ and ψ are studied with the Dirichlet boundary conditions. For function ψ this directly follows from the given non-slip condition. For function ζ we apply a classical *Thom* condition⁹ of Thom which reformulates the conditions for normal derivatives of ψ in terms of a given value of ζ .

Let us first construct Green's functions for ζ and ψ in the reference domain with the trivial boundary conditions on the channel faces and periodic conditions over x . We demonstrate the technique on the simpler case of stream function that implies

$$\begin{aligned} \Delta G_\psi &= \delta(\xi - x) \delta(\eta - y), \quad G_\psi(\xi, 0) = G_\psi(\xi, b) = 0, \\ G_\psi(0, \eta) &= G_\psi(L, \eta), \quad \frac{\partial G_\psi}{\partial \xi}(0, \eta) = \frac{\partial G_\psi}{\partial \xi}(L, \eta). \end{aligned} \quad (3.4)$$

This Green's function can be constructed by expansion in sine trigonometric Fourier series along variable η that automatically provides the trivial boundary conditions over the channel faces. Each Fourier coefficient satisfies a second-order ordinary differential equation with respect to variable ξ whose solution satisfying the periodic conditions is

$$G_\psi = \sum_{m=1}^{\infty} \frac{\sin(b_m \eta) \sin(b_m y)}{\pi m} \frac{e^{b_m |\xi - x|} + e^{b_m (L - |\xi - x|)}}{1 - e^{b_m L}}, \quad b_m = \frac{\pi m}{b}. \quad (3.5)$$

So far as Green's function for function ψ is constructed, the solution to respective Poisson equation for $\psi^{(n)}$ in (3.3) can be written out in explicit form, by using integral Green's theorem:

$$\psi^{(n)}(x, y) = \int_0^L \int_0^b \zeta^{(n)}(\xi, \eta) G_\psi d\xi d\eta. \quad (3.6)$$

The key essence of our method is to use the fact that Green's function provides separation of variables. This permits re-formulation of relation (3.6) for each Fourier component separately:

$$\begin{aligned} \psi_m^{(n)}(x) &= -\frac{1}{2b_m(1 - e^{-b_m L})} \int_0^L [e^{b_m(|\xi - x| - L)} + e^{-b_m|\xi - x|}] \zeta_m(\xi) d\xi, \\ \psi^{(n)}(x, y) &= \sum_{m=1}^{\infty} \psi_m^{(n)}(x) \sin(b_m y), \end{aligned} \quad (3.7a)$$

where

$$\zeta_m^{(n)}(x) = \frac{2}{b} \int_0^b \sin(b_m \eta) \zeta^{(n)} d\eta \quad (3.7b)$$

is again a respective Fourier component of the vorticity.

The second key point of the proposed algorithm is that calculations in (3.7a) require only linear number of arithmetic operations, again thanks to the fact that Green's function representation separates variables not only in vertical but also in the horizontal direction. We can estimate the number of required arithmetic operations to calculate function $\psi^{(n)}(x, y)$. Let us assume that N grid nodes are taken along coordinate x and $M = 2^k$ nodes along coordinate y . If the quantity M is an integer power of 2, then to attain faster computations one can apply FFT to calculate the solution at M points y_m uniformly distributed over the interval $(0, b)$. For each of M Fourier components ($m = 1, 2, \dots, M$) integration in (3.7a), due to separation of variables, requires a linear

number of operations for all $x_j, j=1,2,\dots,N$. It thus requires in total $O(MN)$ arithmetic operations.

It would be interesting to compare this estimate, for example, with analogous estimate if applying FEM. The latter can be reduced to a linear algebraic system with a matrix of the size $MN \times MN$ containing 5 non-zero elements in each line. Some efficient iteration schemes can be applied to solve such a system like a conjugate gradient method, which typically require $O(h^{-1})$ iterations¹⁰. Since each iteration step requires $O(MN)$ arithmetic operations, one can estimate that the FEM implementation requires in total $O(M^2N)$ operations. In the natural case when $N = O(M)$, the number of operations required by FEM grows cubically with the mesh quantity M increasing, but the method proposed here to calculate $\psi^{(n)}(x, y)$ is quadratic over M .

Analogous treatment leads to similar representations for the vorticity. If we construct at first the Green's function G_ζ such that

$$\begin{aligned} G_\zeta - \varepsilon \Delta G_\zeta &= \delta(\xi - x) \delta(\eta - y), \quad G_\zeta(\xi, 0) = G_\zeta(\xi, b) = 0, \\ G_\zeta(0, \eta) &= G_\zeta(L, \eta), \quad \frac{\partial G_\zeta}{\partial \xi}(0, \eta) = \frac{\partial G_\zeta}{\partial \xi}(L, \eta). \end{aligned} \quad (3.8)$$

Then one can obtain, by Fourier sine expansion, the following representation

$$G_\zeta = - \sum_{m=1}^{\infty} \frac{\sin(b_m \eta) \sin(b_m y)}{b \varepsilon \lambda_m} \frac{e^{\lambda_m |\xi - x|} + e^{\lambda_m (L - |\xi - x|)}}{1 - e^{\lambda_m L}}, \quad \lambda_m = \sqrt{b_m^2 + \frac{1}{\varepsilon}}. \quad (3.9)$$

So far as this Green's function is derived, the solution to the first equation in (3.3) can be constructed by applying Green's integral theorem, in the following form

$$\begin{aligned} \zeta_m^{(n)}(x) &= \frac{1}{2\varepsilon \lambda_m (1 - e^{-\lambda_m L})} \int_0^L \left[e^{\lambda_m (|\xi - x| - L)} + e^{-\lambda_m |\xi - x|} \right] g_m^{(n-1)}(\xi) d\xi + \\ &+ \frac{b_m}{b \lambda_m (1 - e^{-\lambda_m L})} \int_0^L \left[\zeta(\xi, 0) - (-1)^m \zeta(\xi, b) \right] \left[e^{\lambda_m (|\xi - x| - L)} + e^{-\lambda_m |\xi - x|} \right] d\xi - \\ &- \varepsilon \int_{\ell} \left(\zeta \frac{\partial G_\zeta}{\partial n} - \frac{\partial \zeta}{\partial n} G_\zeta \right) dl; \quad [\psi^{(n)}, g^{(n)}] = \sum_{m=1}^{\infty} [\psi_m^{(n)}, g_m^{(n)}](x) \sin(b_m y), \end{aligned} \quad (3.10)$$

where ℓ denotes the boundary of the cylinder. Recall that the boundary values for function $\zeta^{(n)}$ are determined, by using Thom approach, through respective values of $\psi^{(n-1)}$ defined from the previous iteration step.

Assume there is no cylinder in the channel, and we wish only to calculate correctly the structure of the turbulent flow incoming. Then the last integral in (3.10) disappears, we it can easily be seen that in this case the number of operations required to implement with formula (3.10) is the same as to perform calculations according to (3.7a), namely $O(MN)$. The only difference here is that in order to know the non-linear term $g_m^{(n-1)}(x)$ for each m and all x_j , this requires to calculate respective Fourier coefficients. By applying an appropriate form of FFT, it takes $O(\log M)$. We just can

conclude that the total number of arithmetic operations in this case is $O(MN \log M)$, slightly higher but in practice the same as the quadratic estimate above.

Now, in the case of round cylinder placed into the turbulent flow, we can see from (3.10) that with a known boundary condition for ζ over ℓ equation (3.10) becomes itself a boundary integral equation for the normal derivative of ζ over the boundary of the cylinder. The length of the cylinder boundary contour has a linear number of grid nodes and requires, for example by using a standard Gauss solver for linear algebraic systems, a cubic number of arithmetic operations. However, in practice the number of nodes over contour ℓ is at least by one order small that the characteristic value of quantities M and N . Therefore, the number of operations required to solve this BIE is of the order of $O(M^3/1000)$, which requires in practice considerably less arithmetic operations than the theoretical estimate $O(MN)$ or $O(MN \log M)$ to calculate (3.7a) and (3.10).

In the conclusion of this section it should be noted that the same approach is applicable in the case if one rejects the periodicity along the horizontal direction and admits instead some other less restrictive conditions, for example, “soft” conditions for the second-order derivatives on the channel entrance and exit.

ACKNOWLEDGEMENTS

The work is partly realized with the support of INTAS (04-80-7043).

REFERENCES

- [1] M.J. Lighthill, “On sound generated aerodynamically. 1. General theory”, Proc. Royal Soc. London, 211A, 564-587 (1952).
- [2] N. Curle, “The influence of solid boundaries on aerodynamic sound”, Proc. Royal Soc. London, 231A, 505-514 (1955).
- [3] Terracol M., Manoha E., Herrero C., Labourasse E., Redonnet S. and Sagaut P. “Hybrid methods for airframe noise numerical prediction”, Theoretical and Computational Fluid Dynamics, 19: 197-227, 2005.
- [4] Desquesnes G., Terracol M., Manoha E. and Sagaut P. “On the use of a high order overlapping grid method for coupling in CFD/CAA”, J. Comput. Phys., 220(1): 355-382, 2006.
- [5] Terracol M., “A Zonal RANS/LES Approach for Noise Sources Prediction”, Flow, Turbulence Combust., 77: 161-184, 2006.
- [6] Desquesnes G., Terracol M. and Sagaut P. “Numerical investigation of the tone noise mechanism over laminar airfoils”, J. Fluid. Mech., in press, 2007.
- [7] Visbal M.R. and Gaitonde D.V. “On use of higher-order finite-difference schemes on curvilinear and deforming meshes”, J. Comput. Phys., 181: 155-185, 2002.
- [8] Kopiev V., Terracol M., Ostrikov N., Zaitsev and Manoha E. “Sound generation by rigid cylinder inserted in flow as a new benchmark problem for airframe noise”, West-East High Speed Flow Field Conference, 2007.

- [9] P.J. Roache, *Computational fluid dynamics*, Hermosa Publ.: Albuquerque, New Mexico, (1976).
- [10] O. Axelsson and A. Barker, *Finite element solution of boundary value problems. Theory and computation*, Academic press: Orlando, Florida, (1984).